Physica C: Superconductivity and its applications 585 (2021) 1353872

Contents lists available at ScienceDirect

Physica C: Superconductivity and its applications

journal homepage: www.elsevier.com/locate/physc

Active vibration control of secondary suspension based on high-temperature superconducting maglev vehicle system

Qingshu Li [a], Zigang Deng [a,b,*], Li Wang [c], Haitao Li [a], Jianghua Zhang [a], Elkin F. Rodriguez [d]

[a] Applied Superconductivity Laboratory, State Key Laboratory of Traction Power, Southwest Jiaotong University, Chengdu 610031, China
[b] Key Laboratory of Magnetic Suspension Technology and Maglev Vehicle, Ministry of Education, Chengdu 610031, China
[c] School of Mechanics and Engineering, Southwest Jiaotong University, Chengdu 610031, China
[d] Electrical Engineering Department, Federal University of Rio de Janeiro, Rio de Janeiro 21941-901, Brazil

ARTICLE INFO

Keywords:
High-temperature superconducting vehicle
Track irregularity
PID control
Fuzzy-PID control

ABSTRACT

The high-temperature superconducting (HTS) magnetic levitation (maglev) vehicle system is a kind of self-stable levitation mode, which is benefited from the characteristic of flux pinning of non-ideal type II superconductor. And this novel prototype has the outstanding advantages of simple structure, reliable principle, friendly environment and so on. But in the HTS maglev vehicle system, the damping coefficients of the primary suspension are very small. The vibration of the YBCO bulks over a permanent magnet guideway (PMG) will be incurred by the fluctuant external magnetic field, which is easily transmitted to the car body to affect the running comfort. The primary goal of this paper is to apply active vibration control into two linear electromagnetic actuators on each bogie. Each electromagnetic actuator is combined with an air spring as a kind of active suspension system in secondary suspension. Initially, the primary suspension stiffness coefficient and damping coefficient of YBCO bulks are measured by experiments. And the mathematical model of HTS maglev vehicle with active actuators was built using the German track spectrum of low interference as PMG irregularity. Then, the dynamic responses of HTS maglev vehicle system were simulated with PID and Fuzzy-PID controllers used in the active actuator to verify the feasibility of the control methods, and compared with the uncontrolled system. Finally, the results of the simulation indicate that both control strategies could improve vehicle comfortable and greatly improve the stability of the system compared to the passive bogie system.

1. Introduction

High-temperature superconducting (HTS) maglev is one of the practical applications of HTS material, which has the characteristics of self-stabilization [1], low energy consumption [2], electromagnetic pollution-free and so on. At present, HTS maglev technology is in the critical stage of commercialization and industrialization, and has high requirements for its safety, stability, and amenity. However, the magnetic inhomogeneity of the permanent magnetic guideway (PMG), crosswind and other factors make the on-board HTS bulks in an alternating magnetic field in the practical operation, which causes the vibration of the HTS maglev system [3-5]. Therefore, increasing system damping scientifically and minimizing the adverse effects of vibration on the system will be essential to improve ride comfort and promote the development of HTS maglev at a higher speed.

To solve this problem, the characteristic research of HTS bulks and its dynamic performance on HTS maglev must be understood. In 1996, Teshima et al. [6] designed a vibration transmissibility measurement apparatus to understand the vibration properties of YBCO bulks, and found that the HTS suspension system is small. Stephan et al. [7] measured the levitation force, the stiffness and the vibration damping of YBCO bulks over two different rail assemblies, and proved that the damping is actually very low in both rails. These confirmed that the HTS maglev system is a weakly damped system, and special damping devices are needed to improve that damping coefficient. Huang et al. [8] studies the relationship between the electromagnetic characteristics and the levitation force of HTS bulks under different field cooling heights (FCH) and working positions based on finite element method, and verified the characteristics among the magnetic flux density on the bottom surface, the internal current density, and the levitation force of HTS bulks through experiments. In order to study the effect of external magnetic field on the dynamic properties of HTS bulks, Hikihara and Moon [9]

* Corresponding author.
E-mail address: deng@swjtu.cn (Z. Deng).

https://doi.org/10.1016/j.physc.2021.1353872
Received 5 March 2021; Received in revised form 9 April 2021; Accepted 15 April 2021
Available online 21 April 2021

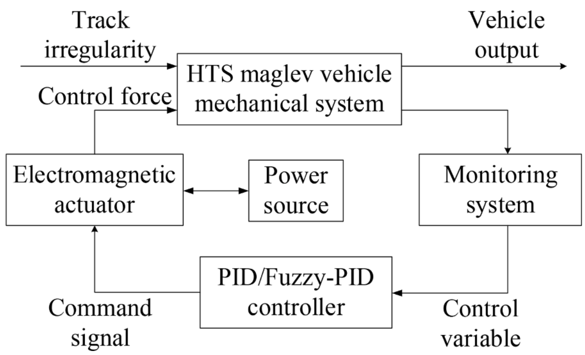

Fig. 1. Layout of active suspension system.

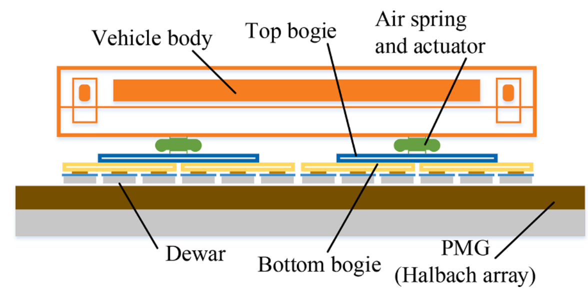

Fig. 2. Schematic of high-temperature superconducting maglev single carriage.

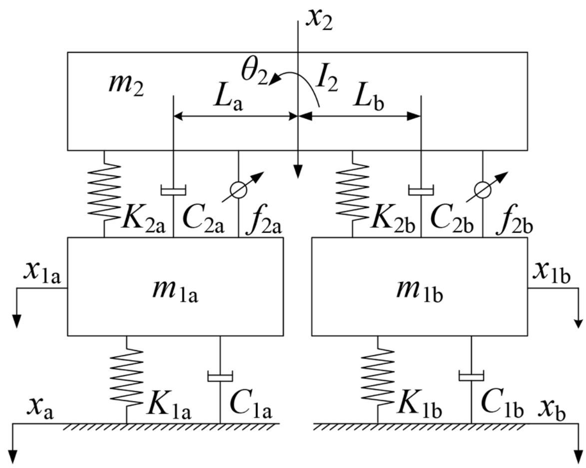

Fig. 3. High-temperature superconducting maglev vehicle model with active actuator.

presented a mathematical model of magnet and superconductor system considering hysteresis effect, studied the motion stability of HTS YBCO bulks on a cylindrical rare earth magnet, analyzed the nonlinear vibration characteristics of HTS bulks, and provide a theoretical basis for the vibration control of HTS maglev. Based on the Hikihara model mentioned above, Pei-Jun Zhuo et al. [10] proposed a new dynamic differential equation of the permanent magnet levitated over a vertically excited HTS bulk, considering the influence of moving speed on the maximum suspension force. Yu et al. [11] designed a new type of EMSD based on the low damping characteristics of HTS maglev and employed to suppress vertical vibration of HTS bulks, and verified the performance of this EMSD at different FCHs by experiments. Sasaki et al. [12,13] proposed a novel electromagnetic shunt damper (EMSD) that is nonlinear coupled with HTS suspension. The induction of this damper can be reduced to a quarter of that of the traditional damper.

Most of the above solutions are aimed at vibration suppression of the primary suspension system of HTS maglev. These methods have a great improvement on the guidance and curve-negotiation behaviors, but it cannot isolate the excitation effectively, so the vibration reduction of the secondary suspension is very important. HTS maglev secondary suspension is mainly used to attenuate the vibration of track irregularities and the static and quasi-static loads transferred from the bogie to the vehicle body. However, the vibration attenuation on HTS maglev secondary suspension has rarely been studied directly. We mostly draw on the active vibration control methods on railway vehicle here. The active control technologies used mainly include Karnoop damping control, linear optimal control, classical PID control, robust control, fuzzy logic control and so on [14]. Fuzzy logic control is especially suitable for nonlinear time-varying and hysteretic systems due to its strong robustness, and has been widely used in active suspension. Sezer and Atalay [15] analyzed the dynamics of a full railway vehicle model with 54 degrees-of-freedom (DOF), and applied fuzzy logic and self-tuning fuzzy control algorithms on control the active controllers placed between vehicle body and bogie to achieve better running performance. Cheng and Li [16] proposed the fuzzy logic control method suitable for a seven DOF full-car model in order to improve the ride comfort, and used the evolutionary programming (EP) method to determine the optimal design parameters of the fuzzy controller. Metin and Guclu [17] used fuzzy logic control and PID control in the secondary suspension of a 2-DOF railway vehicle model to reduce the vibration of body under different track irregularities, and compared time history and frequency response of accelerations and displacements through passive and active controlled system.

This paper builds a 4-DOF HTS maglev vehicle suspension system with a secondary suspension active controller through Simulink. The layout of this active suspension is shown in Fig. 1. The German track spectrum is used as the excitation input of the model [18], and the dynamic response signals of the HTS maglev vehicle are measured by sensors. These monitoring signals will be analyzed by a PID controller or Fuzzy-PID controller to get the desired command signals. Then, commands are transmitted to the electromagnetic actuators to obtain the desired control forces, and finally improve the overall performance of the vehicle system.

2. Modelling of the suspension system

2.1. Mathematical model

Linear electromagnetic actuators are introduced between the vehicle body and bogie frames as force-generating devices in the active suspension model in addition to traditional air springs, which can receive body vibration signals through sensors. The controller controls the force generator to change the stiffness and damping of the suspension system to reduce vibration according to the changes of vehicle driving state and external excitation, therefore obtain good comfort and driving stability. The HTS maglev vehicle model we used here has six Dewars on each bogie and 24 YBCO bulks in each Dewar, as shown in Fig. 2. The bogie is composed of one top bogie and two bottom bogies.

Based on this HTS maglev vehicle, a simplified HTS maglev vehicle model with 4-DOF is shown in Fig. 3. The moments of inertia of m_{1a} and m_{1b} are small, which are not considered here. m_2 is the body mass, m_{1a} is the masses of front bogie and Dewar, m_{1b} is the masses of rear bogie and Dewar, K_{1a} and K_{1b} are stiffness coefficients of suspension force, C_{1a} and C_{1b} are damping coefficients of suspension force, K_{2a} and K_{2b} are stiffness coefficients of air spring, C_{2a} and C_{2b} are damping coefficients of air spring, f_{2a} and f_{2b} are active control forces, x_a and x_b are track irregularity excitation, x_{1a} and x_{1b} are front and rear bogie displacement, x_1 is body centroid displacement, θ_2 is angular displacement of the body, L_a and L_b are distances between bogie and middle of the body, I_2 is the Moment of inertia of the body.

By applying the vehicle vibration model and Newton's second law of motion, the dynamic equations of the suspension system can be written

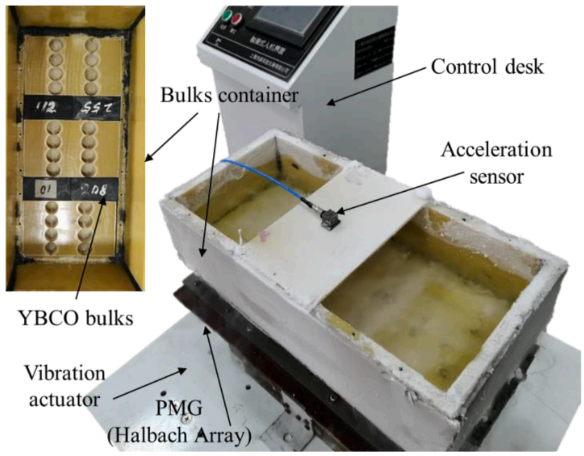

Fig. 4. Experiment setup and the assemble of high-temperature superconducting bulks.

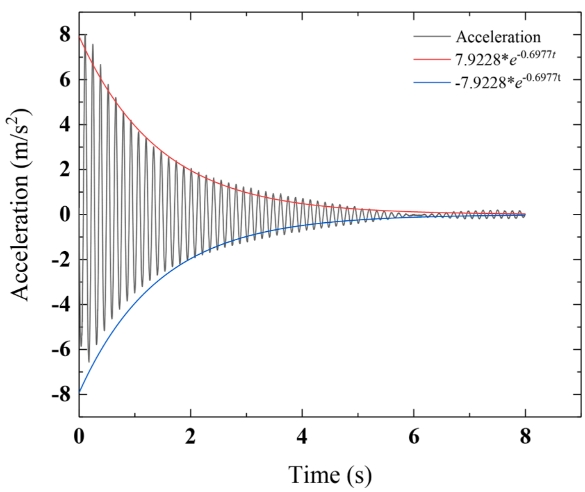

Fig. 5. Free vibration curve with two exponential decay fittings under natural frequency (7.2 Hz).

as follows:

$$m_2\ddot{x}_2 + F_{c2a} + F_{k2a} + F_{c2b} + F_{k2b} - f_{ca} - f_{cb} = 0 \tag{1}$$

$$I_2\ddot{\theta}_2 + L_a(F_{c2a} + F_{k2a} - f_{ca}) - L_b(F_{c2b} + F_{k2b} - f_{cb}) = 0 \tag{2}$$

$$m_{1a}\ddot{x}_{1a} - F_{c2a} - F_{k2a} + F_{c1a} + F_{k1a} + f_{ca} = 0 \tag{3}$$

$$m_{1b}\ddot{x}_{1b} - F_{c2b} - F_{k2b} + F_{c1b} + F_{k1b} + f_{cb} = 0 \tag{4}$$

where F_{k1a} and F_{k1b} indicate suspension stiffness forces; F_{c1a} and F_{c1b} refer to suspension damping forces; F_{k2a} and F_{k1a} represent air spring stiffness forces; F_{c2a} and F_{c2b} are air spring damping forces.

2.2. Measurement of primary suspension stiffness and damping

The primary suspension stiffness and damping of HTS maglev mainly come from the Dewars mounted on the bogie frame. They are affected by sizes and materials of bulks, suspension height, and FCH. The YBCO bucks are provided by the ATZ Company, which are 64 mm in length, 32 mm in width, 13 mm in height. We built an experimental platform to obtain the vertical stiffness and damping coefficients of this kind of bulks, as shown in Fig. 4. This platform is 30 mm FCH and consists of an HTS bulk container with 4 YBCO bulks, a segment of Halbach PMG, an acceleration sensor, and a vertical vibrator. The vibrator gives a slight vertical disturbance to the HTS maglev model and allows it to vibrate freely. Then, the natural frequency and the amplitude attenuation curves of this model are obtained from the signal measured by the acceleration sensor, as shown in Fig. 5. The actual frequency of this system is $f = 7.2$ Hz, and the stiffness coefficient can be considered as $k = 4\pi^2 f^2 m = 6150\mathrm{N/m}$, and the damping coefficient can be obtained from the amplitude attenuation factor $Ae^{-\zeta\omega t}$, which is 4.2 Ns/m. These inherent parameters further prove that the HTS maglev is a low damping system.

2.3. Creation of track excitation signal

Track irregularity is an important external excitation in the operation of HTS maglev. Some defects such as mechanical misalignment, clearance, and exfoliation will produce during the installation of the PMG due to the installation precision, machining error, and other factors, which are the root causes of system vibration. The statistical characteristics of track irregularity can only be obtained by field line measurement and there is no public report to describe the irregularity of PMG surface. The German track spectrum of low interference is used to simulate the permanent magnet track irregularity of the HTS maglev here considering the operation speed of the vehicle (500 km/h) in the simulative calculation.

Vertical profile irregularity of German track spectrum in the spatial domain is:

$$S_v(\Omega) = A_v\Omega_c^{\,2} \Big/ \left(\Omega^2 + \Omega_r^{\,2}\right)\left(\Omega^2 + \Omega_c^{\,2}\right) \quad \mathrm{m}^2 / (\mathrm{rad/m}) \tag{5}$$

where Ω is the spatial angular frequency of track irregularity (rad/m), $\Omega_c = 0.8246$ rad/m and $\Omega_r = 0.0206$ rad/m are the cut-off frequencies, $A_v = 4.032 \times 10^{-7}\mathrm{m}^2\cdot\mathrm{rad/m}$is the roughness coefficient.

The equation of the German track irregularity spectrum S_v (Ω) is related to the spatial angular frequency Ω, and the unit is m^2/(rad/m). For the convenience of subsequent calculation, it is converted into the track irregularity spectrum S_v (f) varying with the spatial frequency f by unit conversion. The unit of S_f (f) is mm^2·m, and the unit of f is m^{-1}. The specific transformation processes are as follows:

$$S_v(f) = 10^6 \cdot 2\pi \cdot S_v(\Omega) \tag{6}$$

$$\begin{aligned} S_v(\Omega) &= \frac{A_v\Omega_c^{\,2}}{(\Omega^2 + \Omega_r^{\,2})(\Omega^2 + \Omega_c^{\,2})} = \frac{2\pi(A_v/2\pi)(2\pi f_c)^2}{\left[(2\pi f)^2 + (2\pi f_r)^2\right]\left[(2\pi f)^2 + (2\pi f_c)^2\right]} \\ &= \frac{(A_v/2\pi)f_c^{\,2}}{2\pi\left(f^2 + f_r^{\,2}\right)\left(f^2 + f_c^{\,2}\right)} \end{aligned} \tag{7}$$

Combining Eqs. (6) and (7),

$$S_v(f) = \frac{10^6 \cdot (A_v/2\pi)f_c^{\,2}}{\left(f^2 + f_r^{\,2}\right)\left(f^2 + f_c^{\,2}\right)} \tag{8}$$

In order to obtain the time-domain sample of track irregularity, the track irregularity spectrum in the spatial frequency domain needs to be transformed into the time-frequency domain through the trigonometric series method [19]. Because the mean square values of these two track spectra are equal in the corresponding bandwidth, so we can get:

$$S_t(f_t)df_t = S_v(f)df \tag{9}$$

where S_t (f_t) is track irregularity spectrum in time-frequency domain (mm^2·s), f_t is the time frequency (Hz).

When HTS Maglev vehicle passes through a wave with a spatial frequency of f at a running speed v, an excitation with a frequency of f_t will be generated, that is, $f_t = v \cdot f$, and we can get:

$$S_t(f_t) = S_v(f)\cdot df \,/\, df_t = S_v\left(\frac{f_t}{v}\right)\cdot df \,/\, dv\cdot f = S_v\left(\frac{f_t}{v}\right) \Big/ v \tag{10}$$

Incorporating Eq. (8) into Eq. (10), the equation of track irregularity

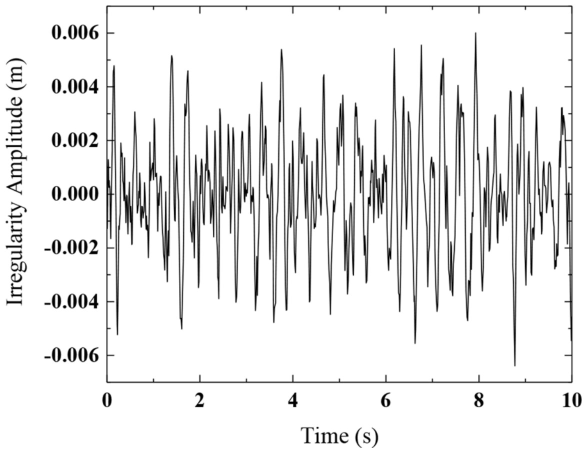

Fig. 6. Time domain sampling of the permanent magnet track guideway.

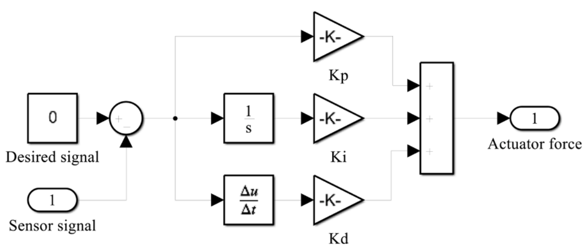

Fig. 7. Simulink simulation model of PID controller.

in the time domain is:

$$S_t(f_t) = \frac{10^6 \cdot (A_v/2\pi) f_c^{\,2} \cdot v}{\left(f_t^{\,2} + f_r^{\,2}\right)\left(f_t^{\,2} + f_c^{\,2}\right)} \tag{11}$$

The time-domain samples are numerically calculated by the Blackman-Turkey method [20], and then the Inverse Fast Fourier Transform (IFFT) is performed to create the time domain samples of track irregularity, as shown in Fig. 6. This track spectrum in time domain is used to predict the response of the vehicle system to the track disturbance and control the suspension system accurately.

3. Controller design

3.1. PID Controller

The PID controller consists of three parts: P (Proportion), I (Integral), and D (Differential). These three parts are constantly adjusted in the process of control to optimize the vertical acceleration of the body [21]. In this study, PID controller was used to controlling the vertical acceleration of the HTS maglev vehicle body directly by taking the difference between the preset value and the real value of the controlled object as signal input, then adjusting three coefficients of the controller to get desired force and reduce the effect of track disturbance on the vehicle body.

The transfer function of the PID controller is described in .Eq. (12)

$$u(t) = K_p e(t) + K_i \int_0^t e(t)dt + K_d \frac{de(t)}{dt} \tag{12}$$

where $e(t)$indicates the difference value between the preset value and the real value of the HTS maglev vehicle body acceleration, $u(t)$refers to the desired output force by PID controller, K_p, K_i and K_d are proportion coefficient, integral coefficient, and differential coefficient respectively.

The PID control model is built in Simulink and combined with the active suspension model as shown in Fig. 7.

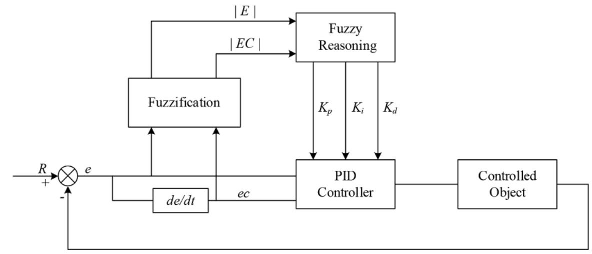

Fig. 8. Layout of fuzzy-PID control.

Table 1.
The fuzzy rule table of ΔK_p, ΔK_i and ΔK_d.

ec	e NH	NM	NS	ZO	PS	PM	PH
NH	H/Z/S	H/Z/S	H/Z/S	H/Z/S	H/Z/S	Z/Z/S	Z/Z/S
NM	H/S/M	M/S/M	M/Z/H	S/Z/H	S/Z/H	Z/S/M	Z/S/M
NS	M/M/Z	M/H/S	S/M/S	Z/H/S	S/H/S	S/M/S	S/M/Z
ZO	M/H/Z	S/H/Z	Z/H/S	Z/H/Z	Z/H/S	S/H/Z	M/H/Z
PS	S/M/Z	S/H/S	S/M/S	Z/H/S	S/H/S	M/M/S	M/M/Z
PM	S/S/M	M/S/M	S/Z/H	S/Z/H	M/Z/H	M/S/M	H/S/M
PH	Z/Z/S	Z/Z/S	H/Z/S	H/Z/S	H/Z/S	H/Z/S	H/Z/S

The abbreviations used correspond to: NH: negative high; NM: negative medium; NS: negative small; ZO: zero; PS: positive small; PM: positive medium; PH: positive high; H: high; M: medium; S: small.; Z: zero.

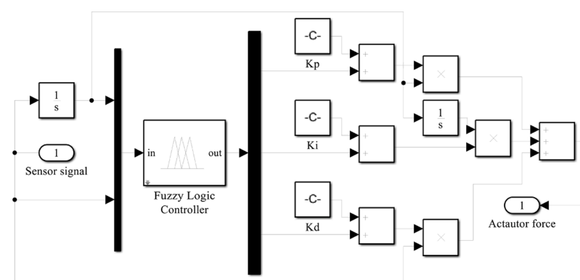

Fig. 9. Simulink simulation model of fuzzy-PID controller.

3.2. Fuzzy PID Controller

The principle of Fuzzy-PID control is shown in Fig. 8. The controller selects the deviation signal *e* of body vertical velocity and the deviation signal *ec* of body vertical acceleration as the inputs to the PID controller and fuzzy controller at the same time. The fuzzy controller obtains correction factors ΔK_p, ΔK_i and ΔK_d after fuzzification, approximate reasoning and defuzzification of the input signals, and combined with PID control parameters to get the desired control force [22].

The adjustment of fuzzy-PID control strategy can reduce the influence of parameter changes in the process of train operation, achieve better control effect and ensure the stableness and security of the train. Based on continuous data processing and theoretical analysis, the relationship among HTS maglev vehicle body vertical velocity deviation *e*, deviating rate *ec* and the control parameters of the regulation ΔK_p, ΔK_i and ΔK_d is as shown in Table 1. based on following rules:

(1) If the absolute value of HTS maglev vehicle body vertical velocity is relatively large, then K_p and K_d should be relatively larger, and K_i should be relatively smaller or 0, in order to accelerate the response of the system and avoid excessive overshoot;
(2) If the absolute value of HTS maglev vehicle body vertical velocity and acceleration is relatively medium, then K_p should take a relatively smaller value, K_i and K_d should be median, in order to reduce the overshoot;

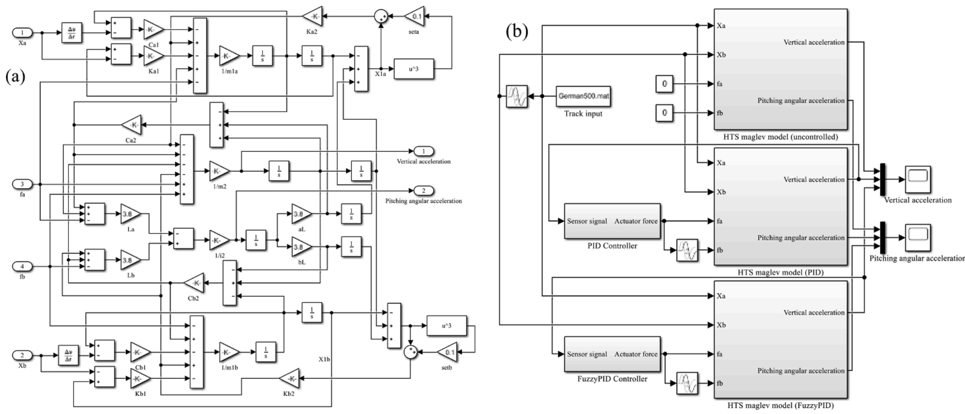

Fig. 10. Simulink simulation structure (a) High-temperature superconducting maglev model; (b) Overall control scheme with PID and fuzzy-PID controller.

Table 2
Simulation parameters of the high-temperature superconducting maglev vehicle.

Parameters	Values
Body mass m_2	8500 kg
Bogie and Dewar mass m_{1a}, m_{1b}	4032 kg
Stiffness coefficient of air spring K_{2a}, K_{2b}	730,000 N/m
Damping coefficient of air spring C_{2a}, C_{2b}	50,000 Ns/m
Stiffness coefficient of suspension force K_{1a}, K_{1b}	3,542,400 N/m
Damping coefficient of suspension force C_{1a}, C_{1b}	2419.2 Ns/m
Relative displacement of bogie and body L_a, L_b	3.8 m
Moment of inertia of body I_2	192,500 kg·m^2

(3) If the absolute value of HTS maglev vehicle body vertical velocity and acceleration is relatively small, then K_p and K_i should be relatively larger, and K_d should be medium or 0, in order to have a good steady-state performance and avoid vibration near the equilibrium point.

The control model is also built in Simulink and combined with the HTS Maglev vehicle model as shown in Fig. 9.

4. Simulation

The HTS Maglev vehicle model is established in Simulink according to the mathematical model represented by Eq. (1)–(4), and taking the German track spectrum as the vertical excitation of the track, as shown in Fig. 10.

The passive bogie, PID control semi-active bogie and fuzzy-PID control semi-active bogie are simulated under the same speed and the same track conditions, and the acceleration and pitch angular acceleration of the body are observed. The stiffness and damping coefficient of the suspension system can be derived from the results of previous experiments, which are 3,542,400 N/m and 2419.2 Ns/m respectively. Other parameters used in the half-vehicle simulation are based on the data of the research group's early dynamics simulation [23]. Each parameter used in the simulation is listed in Table. 2, and the results are shown in Fig. 11.

The root mean square (RMS) values obtained from the simulation data are shown in Table 3.

It can be seen from the results that the RMS values of body acceleration and pitch angular acceleration are optimized by 16.88% and 15.58% respectively under PID control compared with the uncontrolled state, and are optimized by32.40% and 24.68% respectively under fuzzy-PID control. From the results shown above, both two control methods can improve the performance of the HTS maglev vehicle system effectively, and the improvement effects of fuzzy-PID control are higher than that of PID control obviously.

Synthesizing the studies above, a linear electromagnetic actuator mounted on the HTS maglev second suspension is proposed as a special damping device to make up for the low damping coefficient of the system. PID and fuzzy-PID controllers are introduced as the control methods of the actuator. Combined with Simulink, we investigated the dynamic response of the HTS maglev vehicle system at 500 km/h, and proved the effectiveness of these two methods by simulation. Due to the real-time adjustment of parameters, the fuzzy-PID controller has higher fault tolerance to the system and its dynamic responses are also

Table 3.
Root mean square values of the body.

Parameters	Uncontrolled	PID	Fuzzy-PID
Vertical acceleration	0.5260	0.4372	0.3556
Pitch angular acceleration	0.0231	0.0195	0.0174

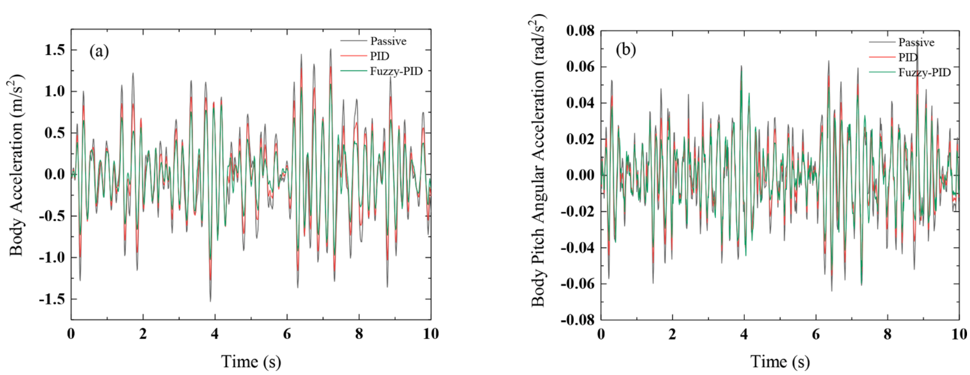

Fig. 11. Vibration response of the vehicle body (a) vertical acceleration; (b) pitch angular acceleration.

significantly higher than the PID controller. Through the vibration control of the secondary suspension, the running safety and riding comfort of the HTS maglev vehicle system are improved obviously.

This work has provided a new idea for the vibration suppression of HTS maglev system, and the practicability was verified preliminarily by simulation.

5. Conclusion

In this paper, an active controller used on HTS maglev is designed in order to increase the damping of the system and enhanced the anti-interference ability of the system. This controller adopted PID and Fuzzy-PID methods respectively, and both achieved the goal of minimizing the track interference of the HTS maglev vehicle model successfully. It can be seen from the results of the study, combining fuzzy control theory and PID control theory is a suitable control method for an active suspension system, which can solve the problem that the single control method is easily affected by uncertain factors, weaken the interference of track irregularity on the system, and improve the ride comfort and operation stability of the HTS maglev system effectively.

This is a very key component in future attempts to increase the stability of the HTS maglev vehicle running at a higher speed. Future research might apply this Fuzzy-PID controller to achieve better ride quality under different speed levels, and this controller can also suppress the lateral disturbance of the vehicle if being used properly.

Author statement

All authors have read and approved to submit it to your journal. There is no conflict of interest of any authors in relation to the submission. This paper has not been submitted elsewhere for consideration of publication.

Declaration of Competing Interest

The authors declare that they have no known competing financial interests or personal relationships that could have appeared to influence the work reported in this paper.

Acknowledgments

This work was partially supported by the National Natural Science Foundation of China (U19A20102, 51875485, 52077178), the Science and Technology Partnership Program, Ministry of Science and Technology of China (KY201701001), the Sichuan Science and Technology Program (21RCYJ0064), the Chengdu International S&T Cooperation Program (2019-GH03-00002-HZ) and the Fundamental Research Funds for the Central Universities (2682020ZT96).

References

[1] J R Hull, Superconducting bearings, Supercond. Sci. Technol. 13 (2) (2000) R1.
[2] F N Werfel, U Floegel-Delor, R Rothfeld, et al., Superconductor bearings, flywheels and transportation, Supercond. Sci. Technol. 25 (1) (2011), 014007.
[3] M Smolyak B, V Ermakov G, I Chubraeva L, The effect of ac magnetic fields on the lifting power of levitating superconductors, Supercond. Sci. Technol. 20 (4) (2007) 406.
[4] W Yang, Y Liu, Z Wen, et al., Hysteresis force loss and damping properties in a practical magnet–superconductor maglev test vehicle, Supercond. Sci. Technol. 21 (1) (2007), 015014.
[5] Y Arai, H Seino, K. Nagashima, Levitation properties of superconducting magnetic bearings using superconducting coils and bulk superconductors, Supercond. Sci. Technol. 23 (11) (2010), 115011.
[6] H Teshima, M Tanaka, K Miyamoto, et al., Vibrational properties in superconducting levitation using melt-processed YBaCuO bulk superconductors, Physica C 256 (1–2) (1996) 142–148.
[7] M Stephan R, R de Andrade Jr, C Dos Santos G, et al., Levitation force and stability of superconducting linear bearings using NdFeB and ferrite magnets, Physica C 386 (2003) 490–494.
[8] H Huang, J Zheng, B Zheng, et al., Correlations between magnetic flux and levitation force of HTS bulk above a permanent magnet guideway, J. Low Temp. Phys. 189 (1) (2017) 42–52.
[9] T Hikihara, C Moon F, Chaotic levitated motion of a magnet supported by superconductor, Phys. Lett. A 191 (3–4) (1994) 279–284.
[10] J Zhuo P, X Zhang Z, F Gou X, Chaotic motion of a magnet levitated over a superconductor, IEEE Trans. Appl. Supercond. 26 (2) (2016) 1–6.
[11] J Yu, Z Deng, H Li, et al., Vibration suppression of high-temperature superconducting maglev system via electromagnetic shunt damper, J. Supercond. Novel Magn. 32 (9) (2019) 2819–2828.
[12] M Sasaki, T. Sugiura, Vibration reduction of rotor supported by superconducting magnetic bearing utilizing electromagnetic shunt damper, IEEE Trans. Appl. Supercond. 26 (3) (2016) 1–4.
[13] M Sasaki, T. Sugiura, Effect of parameters of an electromagnetic shunt damper on whirling amplitude reduction of a rotor supported by a superconducting magnetic bearing, IEEE Trans. Appl. Supercond. 27 (4) (2017) 1–5.
[14] H E Tseng, D. Hrovat, State of the art survey: active and semi-active suspension control, Veh. Syst. Dyn. 53 (7) (2015) 1034–1062.
[15] S Sezer, A E Atalay, Application of fuzzy logic based control algorithms on a railway vehicle considering random track irregularities, J. Vib. Control 18 (8) (2012) 1177–1198.
[16] C P Cheng, T H S Li, EP-based fuzzy control design for an active suspension system with full-car model, in: 2007 IEEE International Conference on Systems, Man and Cybernetics, IEEE, 2007, pp. 3288–3293.
[17] M Metin, R. Guclu, Active vibration control with comparative algorithms of half rail vehicle model under various track irregularities, J. Vib. Control 17 (10) (2011) 1525–1539.
[18] A. Massel, Power spectrum analysis—Modern tool in the study of rail surface corrugations, NDT & E Int. 32 (8) (1999) 429–436.
[19] M Shinozuka, C M Jan, Digital simulation of random processes and its applications, J. Sound Vib. 25 (1) (1972) 111–128.
[20] G Chen, WM. Zhai, Numerical simulation of the stochastic process of railway track irregularities, J. Southwest Jiaotong Univ. 34 (2) (1999) 138–142, in Chinese.
[21] K J Åström, C C Hang, P Persson, et al., Towards intelligent PID control, Automatica 28 (1) (1992) 1–9.
[22] R Guclu, M. Metin, Fuzzy logic control of vibrations of a light rail transport vehicle in use in Istanbul traffic, J. Vib. Control 15 (9) (2009) 1423–1440.
[23] H Wang, Z Deng, S Ma, et al., Dynamic simulation of the HTS maglev vehicle-bridge coupled system based on levitation force experiment, IEEE Trans. Appl. Supercond. 29 (5) (2019), 3601606.